REVIEW

Check for updates

Research progress on the catalytic and thermal decomposition of ammonium dinitramide (ADN)

Yubo Tian,[ab] Weibin Xu,[bc] Weimin Cong,[b] Xueqian Bi,[bd] Jiahui He,[be] Zhe Song,[be] Hongling Guan,*[a] Chuande Huang*[b] and Xiaodong Wang [ID] *[b]

Ammonium dinitramide ($NH_4N(NO_3)_2$, ADN) is regarded as a promising oxidizer due to its low signature and high specific impulse. Generally, ADN undergoes exothermic decomposition above 140 °C accompanied by the byproduct of ammonium nitrate (AN). The inevitable endothermic decomposition of AN decreases the overall heat release, and so there is a need to develop efficient catalysts to guide ADN decomposition along desired pathways with a lower decomposition temperature and higher heat release. A suitable catalyst should be able to withstand the harsh conditions in a thruster to achieve a stable thrust force, which poses a huge obstacle for manufacturing a stable and active catalyst. This review gives a comprehensive summary of the thermal and catalytic decomposition pathways of ADN for the first time, which is expected to deepen the understanding of its reaction mechanism and provide useful guidance for designing prospective catalysts toward efficient ADN decomposition.

1. Introduction

Propellants serve as the power source for rockets and satellite engines, and their decomposition characteristics directly affect the efficiency and survivability of the engine.[1,2] Currently, the

[a]School of Chemical Engineering, Zhengzhou University, Zhengzhou, 450001, P. R. China. E-mail: guanhongling@zzu.edu.cn

[b]CAS Key Laboratory of Science and Technology on Applied Catalysis, Dalian Institute of Chemical Physics, Chinese Academy of Sciences (CAS), Dalian 116023, P. R. China. E-mail: xdwang@dicp.ac.cn; huangchuande@dicp.ac.cn

[c]School of Chemical Engineering, University of Chinese Academy of Sciences, Beijing 100049, P. R. China

[d]College of Environmental Science and Engineering, Dalian Maritime University, Dalian 116026, P. R. China

[e]School of Chemical Engineering, Northwest University, Xi'an 710069, P. R. China

primary focus of researchers is to maximize the energy output of propellants while reducing environmental contamination.[3,4] Ammonium perchlorate (AP) has been widely used as an oxidizer in solid propellants because of its fast-burning rate, high combustion stability, and relatively simple preparation process.[5,6] However, large amounts of hydrogen chloride (HCl) gas could be produced during a space shuttle launch due to the high halogen content, which can react with moisture in the air to form hydrochloric acid that can cause irreversible environmental damage.[7–9] Instead, ammonium nitrate (AN) is considered an alternative to AP due to its low cost, easy preparation, and halogen-free features, yet the relatively low specific impulse and burning rate greatly limit its application.[10,11] As the most widely used liquid monopropellant, hydrazine has been applied in various strategic missiles, rockets, and satellite launching

Yubo Tian received his B.S. degree from Henan Polytechnic University in 2021. Currently, he is an M.S. candidate at the School of Chemical Engineering, Zhengzhou University. His research mainly focuses on the catalytic decomposition of aerospace non-toxic fuels.

Yubo Tian

Weibin Xu received his B.S. degree from China University of Mining and Technology in 2017. Currently, he is a PhD candidate (Joined Study of Master and Doctoral Degree) at the Dalian Institute of Chemical Physics, Chinese Academy of Sciences. His research interests focus on the synthesis technology of ADN and the selective oxidation of methane to oxygenates.

Weibin Xu

systems.[12,13] Nevertheless, hydrazine is highly toxic and can cause severe skin corrosion as well as cancer. Moreover, its strong reducing properties induce an explosion risk and make the propellant prone to be oxidized during the storage and transport process. Therefore, there is an urgent need to develop environmental friendly and high-performance propellants.[14–18]

Ammonium dinitramide (ADN), as a low-sensitivity, high-energy ionic compound, has attracted particular attention since its successful synthesis in 1971.[19,20] Some basic properties of ADN are shown in Table 1. Compared to AP, ADN exhibits significant advantages, including a higher enthalpy of formation, faster-burning rate, higher specific impulse, and no toxic gas HCl is formed during combustion, substantially rendering ADN one of the most promising oxidizers.[21–24] So far, the synthesis processes for ADN are quite mature. Chen et al.[25] summarized several methods (aminopropionitrile method, urea method, carbamate method, and sulfamate method) in their work, which lays the foundation for the scaled-up application of ADN in the future. At first glance, the molecular structure of ADN is simple, being composed of one ammonium cation (NH_4^+) and one dinitramide anion (DN^-). However,

Table 1 Molecular properties of ADN

Characteristics	Parameters
Melting point	93 °C
Enthalpy of formation	-174.3 kJ mol^{-1}
Density	1.812 g cm^{-3}
Molecular weight	124.056 g mol^{-1}
Dissolution enthalpy	140 J g
Oxygen balance	+25.79%
Activation energy	175 ± 25 kJ mol^{-1}
Specific heat capacity	2.35 kJ (K^{-1} kg^{-1})
Saturated vapor pressure	7.78 kPa
Storage temperature	-35–50 °C

detailed structural analysis has suggested that the structure of ADN, analogous to that of dinitraminic acid (HDN), bears two isomers (Fig. 1), including NH_4-$N(NO_2)_2$ with an H-atom of NH_4^+ approaching the N-atom in DN^- (marked as ADN-I) and NH_4-$ON(O)NNO_2$ with a H-atom of NH_4^+ approaching the O-atom in DN^- (marked as ADN-II), co-existing as molecular ADN, and wherein the latter structure gives four different

Weimin Cong is an associate professor at the Laboratory of Catalysts and New Materials for Aerospace, Dalian Institute of Chemical Physics, Chinese Academy of Sciences. He received his PhD degree from the University of Poitiers. His research interests primarily include developing new propellants and catalyzing the decomposition of ADN-based propellants.

Weimin Cong

Chuande Huang received his PhD degree (Industrial Catalysis) from Dalian Institute of Chemical Physics, Chinese Academy of Sciences in 2017. Currently, he is an associate professor at the Laboratory of Catalysts and New Materials for Aerospace, Dalian Institute of Chemical Physics, Chinese Academy of Sciences. His research interests include the catalytic decomposition of ADN-based propellants, the preparation and characterization of perovskite catalysts, and energy and environment-related catalysis.

Chuande Huang

Hongling Guan received her PhD degree (Industrial Catalysis) from Dalian Institute of Chemical Physics, Chinese Academy of Sciences in 2017 and was employed as an associate professor at the School of Chemical Engineering, Zhengzhou University. Her research interests focus on the chemical process optimization, catalyst design, and formulation development of ADN-based propellants.

Hongling Guan

Xiaodong Wang received his PhD (Physical Chemistry/Catalysis) from Dalian Institute of Chemical Physics, Chinese Academy of Sciences in 2000. He has been a professor at Dalian Institute of Chemical Physics since 2007 and a committee member for the Chemical Thermodynamics and Thermal Analysis of Chinese Chemical Society since 2002. Wang focuses on both applied and fundamental research, such as propulsion for vehicles, new catalytic materials for energy conversion, and the application of microcalorimetric technology in catalysis.
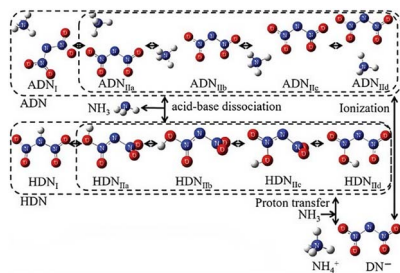
Xiaodong Wang

Fig. 1 Different molecular structures of ADN and HDN. Reprinted with permission from ref. 27. Copyright 2018 Taylor & Francis.

conformers according to the location of O-atom in DN^-.[26,27] These features endow ADN with a complicated decomposition process. Besides, it is worth noting that NH_4^+ in ADN molecules can undergo a hydrolysis reaction with water molecules, leading to strong hygroscopicity and water solubility. Therefore, it is necessary to prevent the deterioration of ADN during its storage process.[28,29]

Solid propellants do not require a complex fuel supply and combustion control systems, which makes solid thrust systems more reliable.[23] As a result, ADN can also be used as an oxidizer and mixed with fuels, binders, and plasticizers to prepare solid composite propellants, which makes it promising to replace the traditional oxidant AP. However, ADN-based solid propellants still have some shortcomings. For instance, the partial intermediate product AN produced during the decomposition process may undergo endothermic decomposition, leading to a reduction in energy release.[30,31] Compared with solid propellants, liquid propellants offer a higher specific impulse while the flow rate and direction of the spray can be precisely regulated, rendering liquid propellants a broader application prospect, such as in satellite attitude regulation and orbital transfer.[32–36] In recent years, various ADN-based liquid monopropellants, as shown in Table 2, have been developed, and among these, propellants (*e.g.*, LMP-103S) with alcohol as the fuel have attracted particular attention due to their outstanding stability and energy intensity.[37,38] However, the currently developed ADN-based liquid monopropellants generally have low sensitivity because of their high-water content, which requires preheating them to a higher temperature for decomposition, meaning they cannot fulfill the requirement of ignition in a short period.[39–41] To solve the problems mentioned above,

incorporating catalysts with good activity and stability is necessary to enable rapid decomposition and the release of more energy by ADN at lower temperature, substantially enhancing the working efficiency of the thruster.

2. Thermal decomposition of ADN

For monopropellants, rapid ignition at lower temperature is the key for propulsion systems. Taking LMP-103S as an example, the decomposition process can be roughly divided into two regions, the decomposition of ADN and the combustion of fuel (*i.e.*, CH_3OH).[42] The decomposition of ADN not only generates the oxidants (*e.g.*, O_2 and NO_2) for the subsequent combustion reaction, but also rapidly increases the temperature of the catalytic bed by releasing heat. Importantly, the specific reaction paths of ADN can be greatly changed by modulating the catalysts, which in turn exerts a significant influence on the ignition process and energy density of the propellant.[43–45] Therefore, clarifying the decomposition mechanisms of ADN and recognizing the corresponding products is of great significance for an ADN-based monopropellant to build reliable combustion models. In addition, the thermal decomposition characteristics can also offer valuable guidance for the catalytic decomposition and engine design. ADN can decompose by different pathways according to the thermal treatment conditions.[46–49] The pioneering research studies have proposed two different ADN decomposition mechanisms: the gas-phase decomposition mechanism and the condensed-phase decomposition mechanism.[50–53]

2.1. Gas-phase decomposition mechanism of ADN

In general, it is believed that ADN will follow the gas-phase decomposition mechanism after sublimation of solid ADN into the gas-state ADN-II.[54,55] The detailed decomposition steps are shown in eqn (1)–(4). This mechanism involves two competing pathways: (1) the gas-state ADN-II obtained after sublimation decomposes into NH_3 and HDN *via* proton transfer (eqn (1)), as shown in Fig. 2. Then the HDN undergoes a molecular rearrangement reaction to form N_2O and HNO_3 (eqn (2)).[56–59] Notably, the molecular rearrangement reaction is relatively complex. It involves the transfer of one $-NO_2$ group from the central N-atom to the O-atoms of the $N-NO_2$ group, which is followed by a further cleavage of the residual N–O bond

Table 2 Composition of some ADN liquid monopropellants

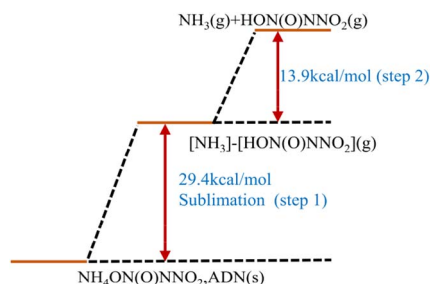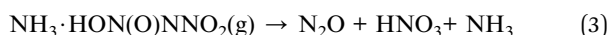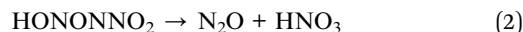| Propellant	Composition		
	ADN (%)	Fuel	Water (%)
LMP-101X	61.0	Glycerol (13.0%)	26.0
LMP-102	58.0	Glycine (16.0%)	26.0
LMP-103X	64.3	Methanol (11.4%)	24.3
LMP-103S	63.0	Methanol (18.4%), aq. ammonia (4.6%)	14.0
FLP-103	63.4	Methanol (11.2%)	25.4
FLP-106	64.6	Monomethylformamide (11.5%)	23.9
FLP-107	65.4	DMF (9.3%)	25.3

Fig. 2 Decomposition characteristics of ADN *via* the gas-phase decomposition mechanism. Reprinted with permission from ref. 57. Copyright 2018 American Chemical Society.

in the central NO_2 motif of $N(O)N–ONO_2$ with the formation of N_2O and NO_3^-. As early as 1997, this pathway was confirmed by Oxley *et al.*[60] *via* ^2H and ^{15}N-labeled ADN at one atmospheric pressure; (2) the other pathway involves the one-step decomposition of gas-state ADN-II into NH_3, HNO_3, and N_2O (eqn (3)).[61] This pathway was confirmed by Fetherof *et al.*[62] in a laser-induced ignition decomposition experiment under one atmospheric pressure. One striking feature of the gas-phase decomposition mechanism is the generation of NH_3 in the first step of the reaction. However, molecular rearrangement can occur in both pathways, leading to the formation of undesired recombination products of AN (eqn (4)).

$$NH_3 \cdot HON(O)NNO_2(g) \rightarrow HONONNO_2 + NH_3 \quad (1)$$

$$HONONNO_2 \rightarrow N_2O + HNO_3 \quad (2)$$

$$NH_3 \cdot HON(O)NNO_2(g) \rightarrow N_2O + HNO_3 + NH_3 \quad (3)$$

$$HNO_3 + NH_3 \rightarrow NH_4NO_3 \quad (4)$$

2.2. Condensed-phase decomposition mechanism of ADN

Unlike the gas-phase decomposition mechanism, ADN in the solid-state or molten-state decomposes directly without sublimation, following the condensed-phase decomposition mechanism.[63–65] The detailed decomposition steps are shown in eqn (5)–(14). Similarly, this mechanism also includes two competitive pathways. One of the pathways undergoes a rearrangement reaction directly, forming AN and N_2O (eqn (5)).[66,67] This pathway was confirmed by Löbbecke *et al.*[68,69] under slow heating under atmospheric pressure conditions. In another pathway, heterolytic or homolytic cleavage of the N–N bond in the DN^- anion occurs with formation of the corresponding ions or free radicals (eqn (6)–(8)). Based on the calculated results of Politzer *et al.*,[70] the energy barrier for the homolytic rapture of N–N bond to form $^\cdot NO_2$ and $NH_4NNO_2^\cdot$ free radicals (eqn (8), 44 kcal mol^{-1}) is much lower than by the heterolytic way (eqn 6, 192.9 kcal mol^{-1} and eqn 7, 249.2 kcal mol^{-1}). Instead, Rahm *et al.*[71] proposed a dimer model to explain the decomposition of the condensed-phase ADN. They concluded that in the structure of ADN_2, NH_4^+ coordinates with one of the NO_2 groups in the DN^- anion, resulting in a strong polarization of the negative

charge toward the coordinated NO_2 group. Furthermore, the N–NO_2 group experiences twisting and elongation. The energy barrier for N–NO_2 group homolysis to $^\cdot NO_2$ is 5.9 kJ mol^{-1} lower than the molecular rearrangement that gives N_2O as the gaseous product, as shown in Fig. 3. In 2017, Izato *et al.*[27,72] presented a detailed chemical kinetics model for the molten-state free-radical reactions of ADN based on quantum chemical calculations. They concluded that the decomposition of ADN begins with the homolysis of N–NO_2 in the isomer (ADN-II), see eqn (9). Subsequently, $NNO_2NH_4^\cdot$ dissociates into N_2O, NH_3, and $OH^\cdot$ (eqn (10)). The $OH^\cdot$ then reacts with $NO_2^\cdot$ to form HNO_3 (eqn (11)), whereas NH_3 and HNO_3 recombine to produce AN (eqn (12)). The entire decomposition process can be regarded as the decomposition of ADN-II into N_2O and AN (eqn (13)). Alavi *et al.*[20] conducted detailed calculations of the energy barriers of several possible decomposition pathways of solid-state ADN. Their results showed that the energy barriers for ADN decomposition to N_2O (eqn (5)) and $^\cdot NO_2$ (eqn (8)) in a single step are 35.2 and 35.4 kcal mol^{-1}, respectively. Besides, the direct decomposition of solid ADN into NH_3 and AN (eqn (14)) was also calculated, and it was found that the energy barrier for this reaction was in the range of 30–44 kcal mol^{-1}. Consequently, they concluded that NH_3 can be directly released in the early stage of ADN decomposition, but the main gas product is still N_2O. Currently, the condensed decomposition model suggests that the first step of ADN decomposition mainly involves molecular rearrangements and free-radical reactions. The main gas product is N_2O, with NH_3 being produced in large quantities only in the middle and late stages of the reaction.
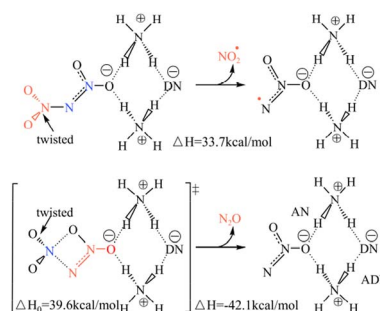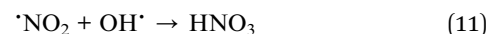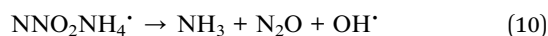
$$NH_4^+N(NO_2)_2^+ \rightarrow NH_4^+NO_3^- + N_2O \quad (5)$$

$$NH_4^+N(NO_2)_2^+ \rightarrow NH_4^+NNO_2^{2-} + NO_2^+ \quad (6)$$

$$NH_4^+N(NO_2)_2^+ \rightarrow NH_4^+NNO_2 + NO_2^- \quad (7)$$

$$NH_4^+N(NO_2)_2^+ \rightarrow NH_4^{+\cdot}NNO_2^- + ^\cdot NO_2 \quad (8)$$

$$ADN\text{-}II \rightarrow NNO_2NH_4^\cdot + ^\cdot NO_2 \quad (9)$$

$$NNO_2NH_4^\cdot \rightarrow NH_3 + N_2O + OH^\cdot \quad (10)$$

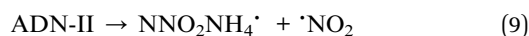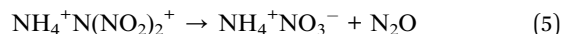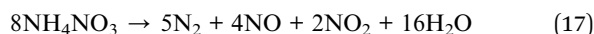$$^\cdot NO_2 + OH^\cdot \rightarrow HNO_3 \quad (11)$$

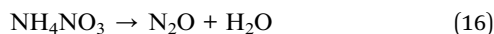**Fig. 3** Decomposition model of the ADN dimer. Reprinted with permission from ref. 71. Copyright 2009 Royal Society of Chemistry.

$$NH_3 + HNO_3 \rightarrow NH_4NO_3 \quad (12)$$

$$ADN\text{-}II \rightarrow N_2O + NH_4NO_3 \quad (13)$$

$$NH_4{}^+N(NO_2)_2{}^+ \rightarrow HN(NO_2)_2 + NH_3 \quad (14)$$

According to the decomposition mechanisms in the gas phase and condensed phase, the intermediate AN will inevitably be formed during the thermal decomposition of ADN.[73–76] Numerous studies have shown that AN decomposition occurs at above 170 °C through different pathways (eqn (15)–(17)).[77–80] At temperatures below 260 °C, AN primarily undergoes endothermic decomposition to produce NH_3 and HNO_3 following eqn (15). Above 260 °C, AN decomposes along eqn (16) and (17) with the release of a substantial amount of heat, which is preferred in practical application.

$$NH_4NO_3 \rightarrow NH_3 + HNO_3 \quad (15)$$

$$NH_4NO_3 \rightarrow N_2O + H_2O \quad (16)$$

$$8NH_4NO_3 \rightarrow 5N_2 + 4NO + 2NO_2 + 16H_2O \quad (17)$$

3. Catalytic decomposition of ADN

With an aim to make ADN decompose at a lower temperature, maximize the energy release, and enhance the efficiency of thrust, catalytic ADN decomposition has aroused notable research attention. This chapter provides a summary of the recent research progress in the catalytic decomposition of ADN, aiming to offer insights into the reaction mechanism and provide guidance for designing efficient catalysts.

3.1. Evaluation methods

The selection of an appropriate evaluation method is crucial for screening high-performance catalysts. Currently, there are three methods commonly used for performance evaluation.

(1) TG-DSC or TG-DTA. As a commonly used physical property analysis technique, the heat flow and weight change of a material with temperature can be recorded over time to determine the composition and state of the material. When used for assessing the catalytic decomposition of ADN, the catalytic effect on the thermodynamic and kinetic features of the decomposition process can be assessed by examining factors such as the decomposition rate, heat release magnitude, onset of decomposition temperature, and location of the peak temperature. This information can be used to evaluate the catalytic activity and infer the reaction mechanism.[81–83]

(2) Batch catalytic reactor. This mainly comprises a closed vessel and a feeding needle, operating at a pressure between 0 to 5 bar. The structure is roughly depicted in Fig. 4a. The main advantages of the batch reactor include the ability to preheat the catalyst bed and enable real-time monitoring of the reactor pressure, state of catalyst, and gas-phase temperature. In the realm of catalytic ADN decomposition, this setup is suitable for
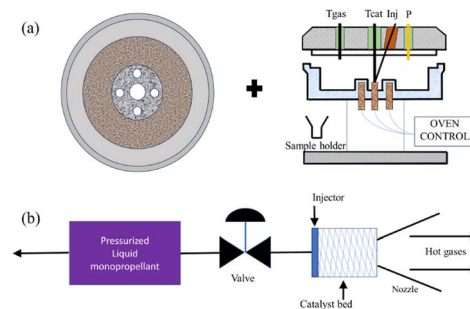

Fig. 4 Schematic diagrams of (a) batch catalytic reactor structure. Reprinted with permission from ref. 84. Copyright 2003 American Institute of Aeronautics and Astronautics, and (b) self-designed simulation thruster. Reprinted with permission from ref. 90. Copyright 2014 Springer.

evaluating parameters such as the catalytic decomposition rate, ignition delay, and onset of ADN decomposition temperature.[84–87]

(3) Self-designed simulation thruster. This mainly consists of a combustion chamber, nozzle, control system, and cooling system, as shown in Fig. 4b, which initiates the decomposition reaction by passing the propellant through a preheated catalytic bed. This reaction breaks down large molecule compounds into small molecule compounds, accompanied by the release of a substantial amount of heat.[88,89] The high-temperature and high-pressure gases generated after the reaction are expelled from the nozzle. This thruster is commonly used to test the high-temperature stability of the catalyst and to simulate the catalytic combustion state of ADN in a real application environment.[90,91]

3.2. Catalytic activity

Currently, the reported catalysts for ADN decomposition can be classified into noble metal catalysts and non-noble metal catalysts. The catalytic activity and corresponding evaluation methods of some catalysts are shown in Table 3.

3.2.1 Non-noble metal catalysts. Non-noble metal catalysts typically utilize transition metals (Fe, Co, Cu, *etc.*) or non-metallic elements (N, C, *etc.*) as active centers. They can reduce the cost and reliance on noble metals in the catalytic industry.[102–104]

These catalysts generally play a role in reducing the activation energy and accelerating proton transfer when catalyzing ADN decomposition. Zhai *et al.*[92] analyzed DSC curves obtained at different heating rates and calculated the activation energies for ADN catalytic decomposition using the Kissinger method. The results indicated that the addition of 5% $PbCO_3$ reduced the activation energy from 179 kJ mol^{-1} to 165 kJ mol^{-1}, and the onset decomposition temperature of ADN decomposition was lowered by 10 °C based on the DSC analysis. Li *et al.*[93] investigated the catalytic decomposition behavior of CNTs and Fe_2O_3/CNTs using TG. The experimental results revealed that the inclusion of CNTs led to a notable weight loss of ADN at an earlier stage while the catalytic activity declined upon the

Table 3 Summary of the catalytic performance of some noble metal and non-noble metal catalysts[a]

Catalysts	Evaluation method	Thermal decomposition		Catalytic decomposition		Ref.
		T_{onset}/°C	T_{peak}/°C	T_{onset}/°C	T_{peak}/°C	
PbCO$_3$	TG-DSC	173.7		158.3		92
CNTs	TG-DTA	168.9		150.6		93
Fe$_2$O$_3$/CNTs	TG-DTA	168.9		156.8		93
Nano-Co	TG-DSC		200.05		178.7	94
Co/CuCr$_2$O$_4$	DSC		185		136	95
Ba/CuCr$_2$O$_4$	DSC		185		137	95
CuO	TG-DTA	157		117		96
CuO	SC-DSC		about 180	about 150		97
CuO	TG-DTA		185.49		141	98
Pt–Zn/Al$_2$O$_3$	TGA-DTA		176		147	90
Pd/Al$_2$O$_3$	TGA-DTA		181		147	99
Pt–Cu/LHA	TG-DSC		175		129	100
Pt–Cu/LHA	Batch reactor	134		105		101
Ir/Al$_2$O$_3$	Batch reactor	190		184		87
Ir/La–Al$_2$O$_3$	Batch reactor	190		182		87
Ir/Si–Al$_2$O$_3$	Batch reactor	190		189		87

[a] T_{onset} and T_{peak} represent the onset decomposition temperature and temperature at the highest point of the ADN exotherm, respectively.

introduction of Fe$_2$O$_3$. Therefore, they concluded that CNTs could offer additional adsorption and desorption sites for ADN due to their larger cavity structure, contributing to the initial decomposition process. Duan et al.[94] found that introduction of 5% Co powder in ADN could shift the decomposition peak to lower temperature by approximately 22 °C, accompanied by a slight increase in the apparent exothermic behavior. They suggested that the Co catalyst can accept a lone pair from the NH$_3$ ligand, which reduces the concentration of NH$_4^+$ and accelerates proton transfer. Shamjitha et al.[95] prepared Co- and Ba-doped CuCr$_2$O$_4$ catalysts via hydrothermal method and evaluated their performance for the decomposition of aqueous ADN solution and ADN-based monopropellant (LMP103X). They found that these two catalysts displayed similar activity, which could lower the peak decomposition temperature of ADN by ca. 50 °C, while the addition of methanol (LMP103X) exerted negligible influence on the decomposition of ADN. The mechanism investigation showed that the introduction of Ba or Co into CuCr$_2$O$_4$ could promote the concentration of the active sites (e.g., Co^{2+}, Cu^{2+}, and Cr^{3+}) and oxygen vacancies, which facilitated the adsorption and decomposition of ADN.

CuO has attracted particular attention due to its outstanding performance. Fujisato et al.[96] found that CuO could lower the onset decomposition temperature of solid ADN from 157 °C to 117 °C. A mechanism study showed that CuO could react with ADN to form the corresponding copper complexes, which accelerated the decomposition of ADN. Based on sealed cell differential scanning calorimetry (SC-DSC) analysis, Matsunaga et al.[97] observed a similar phenomenon. They found that the peak temperature of ADN decomposition was reduced under the catalysis of CuO, and that the overall reaction proceeded as a one-step exothermic process, as shown in Fig. 5. Additionally, CuO also underwent a color change process, starting as black, then turning bluish-green, and finally returning to black. Combining FTIR and MS, they proposed a relatively detailed

catalytic mechanism; whereby, upon the activation of CuO, ADN undergoes initial dissociation, forming NH$_3$ and HDN. Following this, HDN reacts with CuO to produce Cu(NO$_3$)$_2$, NO$_2$, and H$_2$O during the early stage of decomposition (eqn (18)). Then, a portion of Cu(NO$_3$)$_2$ reacts with NH$_3$, producing NO$_2$, N$_2$, and H$_2$O (eqn (19) and (20)), eventually, these copper complexes undergo decomposition, forming the initial CuO (eqn (21)). Gugulothu et al.[98] found that hydrogen bonds or coordination interactions are formed between ADN and CuO through surface Lewis-acid sites. This facilitates the initial dissociation of ADN molecules. The subsequent reaction between HDN and CuO produces NO$_2$, which exhibits autocatalytic effects, enhancing the overall reaction rate of the system. A simplified decomposition schematic diagram is shown in Fig. 6. Based on the condensed-phase decomposition mechanism, ADN inevitably generates a significant quantity of AN during the thermal decomposition process, which will absorb heat to form NH$_3$ and HNO$_3$.[105,106] However, in the experiments of Gugulothu et al.,[98] the endothermic peak resulting from the
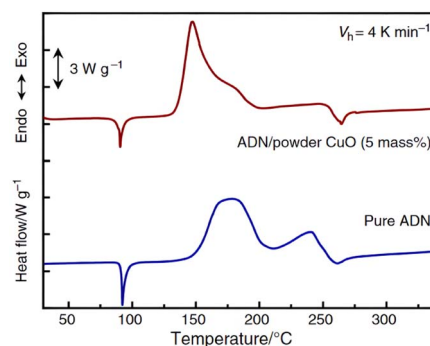

Fig. 5 SC-DSC plots and decomposition activation energy curves of pure ADN. Reprinted with permission from ref. 97. Copyright 2015 Springer.
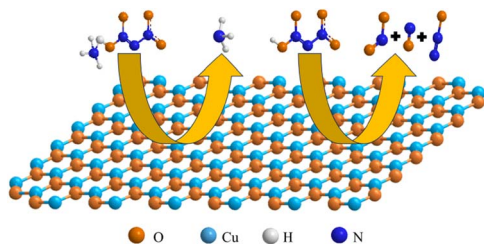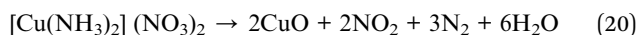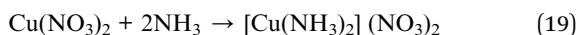
Fig. 6   Schematic diagram of ADN adsorption decomposition on CuO.

decomposition of AN was not observed. In this regard, the researchers proposed that CuO can also alter the decomposition pathways of ADN.[105–107]

$$2HN(NO_2)_2 + CuO \rightarrow Cu(NO_3)_2 + 2NO_2 + H_2O \quad (18)$$

$$Cu(NO_3)_2 + 2NH_3 \rightarrow [Cu(NH_3)_2](NO_3)_2 \quad (19)$$

$$[Cu(NH_3)_2](NO_3)_2 \rightarrow 2CuO + 2NO_2 + 3N_2 + 6H_2O \quad (20)$$

$$Cu(NO_3)_2 \rightarrow 2CuO + 4NO_2 + O_2 \quad (21)$$

3.2.2   Noble metal catalysts. Due to the unique electronic states of noble metals, these catalysts normally display a catalytic performance superior to non-noble metal catalysts.[108–110] In addition, the high melting point of noble metals endows these catalysts with better sintering resistance. Therefore, noble metals are widely used in the aerospace industry for catalytic applications.

As early as 2008, Farhat et al.[111] discovered that when catalyzed by a Pt/Si–Al$_2$O$_3$ catalyst, increased heat release was achieved from ADN decomposition with the generation of more N$_2$O. Accordingly, they proposed that a large amount of AN intermediate will be formed during ADN decomposition. To verify this deduction, they further studied the decomposition behavior of AN by DTA-TGA. The results showed that AN undergoes endothermic decomposition (eqn (16)) at 246 °C. However, when catalyzed by the Pt/Si–Al$_2$O$_3$ catalyst, AN exhibited significant exothermic decomposition at approximately 170 °C. Therefore, they concluded that Pt can alter the decomposition path of AN, substantially improving the macroscopic heat release.[112] Similarly, Batonneau et al.[90] also found that ADN displays a concentrated exothermic behavior over the Pt–Zn/Al$_2$O$_3$ catalyst while there is a significant reduction in the decomposition temperature. Lu et al.[99] found that the Pd/Al$_2$O$_3$ catalyst could reduce the decomposition peak temperature of ADN from 181 °C to 147 °C, showing one-step exothermic decomposition that is similar to Pt. Baek et al.[100] prepared a kind of Pt–Cu/LHA catalyst by depositing Pt and Cu onto La-hexaaluminates and showed that the peak decomposition of ADN monopropellant (LMP-103S) was notably reduced from 175 °C (no catalyst) to 129 °C. Maleix et al.[101] also found that the onset temperature for LMP-103S decomposition declined from 134 °C (no catalyst) to 105 °C, which highlighted the high activity of the Pt–Cu alloy in this reaction.

A detailed study of Ir-based catalysts for ADN decomposition was carried out by Kurt et al.,[87] wherein the catalysts were prepared by loading Ir on undoped and doped Al$_2$O$_3$ (using La and Si) via the termed RR method (reduction of the catalyst precursor with hydrogen) and CRR method (the catalyst precursor is calcined in air and then reduced by hydrogen), respectively. Based on the results from a batch reactor evaluation, they observed that the decomposition of ADN could be notably enhanced over a Si-doped catalyst. Combined with in situ CO-FTIR (Fig. 7a) and XAFS (Fig. 7b) characterization, they concluded that the SiO$_x$–AlO$_x$ structure will be formed after the carrier is doped with Si, which exhibits a strong interaction with the active metal Ir, leading to an increased generation of Ir^{x+} species. These Ir^{x+} species facilitate the adsorption of ADN on the Ir^{x+} sites, promoting ADN decomposition and promoting a rapid decomposition of the intermediate to release more gaseous products NH$_3$ and N$_2$O. In contrast, the interaction between Ir- and La-doped or undoped carriers is weak, wherein Ir exists predominantly as Ir^0 nanoparticles on the carriers. Also, the products of ADN decomposed on Ir^0 (NP) are easily desorbed, thereby showing a lower onset decomposition temperature.

Overall, noble metals, such as Pt, Pd, and Ir, can effectively promote the decomposition rate of ADN and reduce the reaction temperature. However, most researchers tend to mainly focus on the catalytic activity while the structure–function relationship remains ambiguous, which is mainly ascribed to the complex reaction mechanism.

3.3.   Selection of carriers for ADN-based monopropellant liquid propellant decomposition

ADN decomposition is a violent exothermic reaction, rendering a catalytic bed temperature generally higher than 1200 °C.[113,114] Therefore, the selection of a suitable support for the catalysts is of great significance for manufacturing a stable catalyst. Al$_2$O$_3$ is
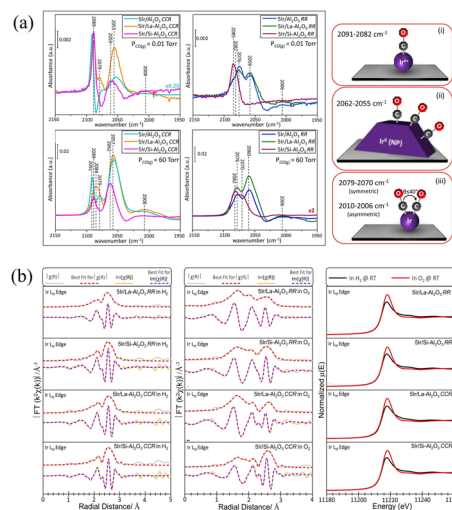

Fig. 7   (a) In situ FTIR spectra and CO vibrational features for the catalysts upon CO adsorption. (b) In situ XAFS data of the catalysts. Reprinted with permission from ref. 87. Copyright 2022 Elsevier.

widely employed as a support for the decomposition of hydrazine and ADN due to its outstanding mechanical strength.[101] However, Al_2O_3 has multiple crystalline phases, which tend to sinter and transform into the alpha phase with a lower specific surface area above 1000 °C. This transformation can negatively impact the catalytic performance, leading to a reduction in catalytic activity.[115,116] To further enhance the mechanical strength of the catalyst and withstand the complex conditions in the thrust, Al_2O_3 materials doped with modifications and hexaaluminates have gradually attracted focus from researchers.

Previous studies have reported that La and Si could change the electronic structure of platinum group metals on Al_2O_3 and enhance the dispersion of active sites on the carrier surface. Additionally, both La and Si can effectively promote the stability of Al_2O_3 at high temperatures.[117–120] Maleix et al.[121] synthesized a Pt–Cu/Si–Al_2O_3 catalyst through the sol–gel method, employing Pt–Cu as the active metal and tetraethoxysilane as the silicon precursor. The catalyst reduced the decomposition temperature of ADN-based monopropellant (FLP-106) from 148 °C to 97 °C. Moreover, the specific surface area of the doped carrier was tested and found to remain around 9 m^2 g^{-1} after treatment at 1350 °C for 2 h, which implied that the catalyst could achieve longer catalytic stability below 1200 °C. To further enhance the overall mechanical strength and high-temperature stability of the catalysts, Kim et al.[122] coated a mixed slurry of Cu $(NO_3)_2 \cdot 3H_2O$ and La-doped Al_2O_3 on the supporting material $5SiO_2–2MgO–2Al_2O_3$. Subsequently, the mixture was subjected to calcination at 1200 °C, resulting in the formation of a highly heat-resistant Cu–La–Al/honeycomb catalyst. The catalyst could reduce the onset decomposition temperature of the ADN-based monopropellant by about 20 °C. Furthermore, with the support of $5SiO_2–2MgO–2Al_2O_3$, the catalyst consistently maintained high stability at 1200 °C.

Furthermore, MP-structured hexaaluminates consisting of La/Sr exhibited superior heat resistance compared to traditional Al_2O_3. It was reported that they could maintain a high specific surface area of 20 m^2 g^{-1} even after exposure at 1200 °C for 4 h.[123] As a result, these hexaaluminates are usually employed as carriers for active metals in catalyzing the decomposition and combustion of ADN.[124–127] Jo et al.[128] loaded Pt on $Sr_{0.8}La_{0.2}MnAl_{11}O_{19}$ by the immersion method followed by calcination at 550 °C and 1200 °C to obtain Pt/hexaaluminate catalysts, respectively. According to the experimental results, the catalysts exhibited similar catalytic activity, and both could reduce the onset decomposition temperature of ADN-based monopropellant by 65 °C in a batch reactor. This was due to the $Sr_{0.8}La_{0.2}MnAl_{11}O_{19}$, which exhibited a higher sintering resistance and could maintain the stability of the catalyst structure even after calcination at a high temperature of 1200 °C, resulting in their similar catalytic activities. This idea was verified by Hong et al.[129] under the same experimental conditions. Heo et al.[130] deposited Cu in the $Sr_{0.8}La_{0.2}MnAl_{11}O_{19}$ bulk phase by a coprecipitation method. A binder was added to produce Cu/hexaaluminate pellets via high-temperature calcination at 1200 °C for the catalytic decomposition of ADN-based liquid monopropellant. The results indicated that the catalyst

significantly lowered the onset decomposition temperature of ADN-based propellant from 167.6 °C to 93.8 °C. Additionally, to test the heat resistance of the catalyst, they repeatedly heat-treated the catalyst at 1200 °C for 10 min, and tested the performance of the catalyst after each heat shock. The results showed that the catalytic activity of the catalyst remained stable after repeating the experiment for 5 times, as shown in Fig. 8. In summary, Al_2O_3 doped with Si and La, as well as MP-structured hexaaluminates, exhibit superior heat resistance compared to regular Al_2O_3. These materials can serve as excellent catalyst carriers for the decomposition and combustion of ADN-based monopropellants.

4. Perspectives

ADN is a novel oxidizer that possesses the virtues of a high energy density and low toxicity. These endow it with promising prospects and practical potential for future rocket and space technology.

The thermal decomposition pathways of ADN are complex and produce various products, including N_2O, NO_2, N_2, NH_3, and NO. To improve fuel efficiency and power output, researchers have devoted much effort to designing suitable catalysts with the aim to release more heat along exothermic pathways at lower temperatures. It is known that Cu-based catalysts can alter the decomposition pathways and significantly reduce the decomposition temperature of ADN. However, the melting point of reduced Cu is 1085 °C and may be deactivated by a loss of the active components in high-temperature applications. It is reported that alloying has the advantages of promoting high thermal strength and chemical activity.[131,132] In follow-up research, non-noble metal alloys could be developed to improve the catalyst performance and reduce the cost of the catalyst. In contrast, noble metal catalysts based on Ir, Pt, and Pd show excellent catalytic activity for the decomposition of ADN. Moreover, noble metals have high melting points (generally above 2000 °C) and are not easily deactivated in high-temperature reactions. Therefore, noble metals currently dominate in aerospace catalytic applications. However, the current research still has several limitations, since the understanding of ADN decomposition mechanisms is limited to
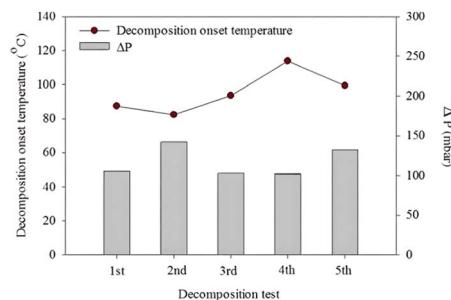

Fig. 8 Onset decomposition temperature and pressure drop during the decomposition of ADN-based monopropellant over Cu/hexaaluminate for five repetitive tests with thermal shock. Reprinted with permission from ref. 130. Copyright 2019 Springer.

analyzing the macroscopic decomposition products and exotherms. More detailed analysis of the adsorption state, and decomposition mechanisms of ADN and blended ADN, such as mixtures of ADN and alcohol, on the catalyst is still unclear. There is an urgent need for *in situ* or *operando* techniques to gain insights into the reaction mechanism.

Although much progress has been achieved these years, the blended ADN monopropellant still suffers from the problem of poor ignition stability due to catalyst deactivation at high temperatures.[41,133] Therefore, studies exploring alternative ignition methods, such as pilot flame igniter ignition, glow plug ignition, microwave controlled ignition, resistive ignition, and laser ignition, would be of great significance for extending the working life of the engine and improving its operational stability.[134–136] In practical applications, utilizing efficient ignition methods can greatly reduce the amount of propellant consumed for preheating while improving the engine's ability to respond to emergencies during that operation. This is of great significance for extending the working life of the engine and improving its operational stability. Besides, pioneering reports validated that the composition of monopropellant (*e.g.*, ADN/methanol ratio and type of added fuel), catalytic bed structure, and operation parameters all play essential roles in the combustion of ADN-based liquid propellants. A comprehensive study on these parameters could accelerate the pace of these monopropellants being applied in practical applications.[34,42,137]

Conflicts of interest

There are no conflicts to declare.

Acknowledgements

References

1 A. Okninski, J. Kindracki and P. Wolanski, *Aerosp. Sci. Technol.*, 2018, **82–83**, 284–293.

2 T. W. Khan and I. Qamar, *Acta Astronaut.*, 2020, **176**, 1–12.

3 R. Armstrong, B. Baschung, D. Booth and M. Samirant, *Nano Lett.*, 2003, **3**, 253–255.

4 H. M. Li, G. X. Li, L. Li, J. Z. Wu, Z. P. Yao and T. Zhang, *Fuel*, 2023, **344**, 128142.

5 P. Zhou, S. Zhang, Z. Ren, X. Tang, K. Zhang, R. Zhou, D. Wu, J. Liao, Y. Zhang and C. Huang, *Adv. Sci.*, 2022, **9**, 2204109.

6 L. Y. Zhou, S. B. Cao, L. L. Zhang, G. Xiang, X. F. Zeng and J. F. Chen, *ACS Appl. Mater. Interfaces*, 2022, **14**, 3476–3484.

7 T. T. Vo, D. A. Parrish and J. M. Shreeve, *J. Am. Chem. Soc.*, 2014, **136**, 11934–11937.

8 Q. Chu, M. Wen, X. Fu, A. Eslami and D. Chen, *J. Phys. Chem. C*, 2023, **127**, 12976–12982.

9 M. Nourine, M. K. Boulkadid, S. Touidjine, H. Akbi and S. Belkhiri, *Mater. Chem. Phys.*, 2023, **303**, 127784.

10 Q. Duan, H. Cao, X. Li and J. Sun, *Process Saf. Environ. Prot.*, 2023, **171**, 482–492.

11 V. Babrauskas and D. Leggett, *Fire Mater.*, 2020, **44**, 250–268.

12 A. S. Yang and T. C. Kuo, *J. Propul. Power*, 2002, **18**, 270–279.

13 D. I. Han, C. Y. Han and H. D. Shin, *J. Spacecr. Rockets*, 2009, **46**, 1186–1195.

14 R. L. Sackheim and R. K. Masse, *J. Propul. Power*, 2014, **30**, 265–276.

15 H. N. Nguyen, J. A. Chenoweth, V. S. Bebarta, T. E. Albertson and C. D. Nowadly, *Mil. Med.*, 2021, **186**, e319–e326.

16 J. K. Niemeier and D. P. Kjell, *Org. Process Res. Dev.*, 2013, **17**, 1580–1590.

17 V. Matyshak and O. Silchenkova, *Kinet. Catal.*, 2022, **63**, 339–350.

18 R. Amrousse, T. Katsumi, N. Azuma and K. Hori, *Combust. Flame*, 2017, **176**, 334–348.

19 S. Venkatachalam, G. Santhosh and K. Ninan Ninan, *Propellants, Explos., Pyrotech.*, 2004, **29**, 178–187.

20 S. Alavi and D. L. Thompson, *J. Chem. Phys.*, 2003, **119**, 232–240.

21 M. Y. Nagamachi, J. I. S. Oliveira, A. M. Kawamoto and R. d. C. L. Dutra, *J. Aerosp. Technol. Manage.*, 2009, **1**, 153–160.

22 I. I. Sam, S. Gayathri, G. Santhosh, J. Cyriac and S. Reshmi, *J. Mol. Liq.*, 2022, **350**, 118217.

23 S. Sims, S. Fischer and C. Tagliabue, *Propellants, Explos., Pyrotech.*, 2022, **47**, e202200028.

24 R. Amrousse, T. Katsumi, N. Azuma, K. Hatai, H. Ikeda and K. Hori, *Sci. Technol. Energ. Mater.*, 2016, **77**, 105–110.

25 F. Chen, C. Xuan, Q. Lu, L. Xiao, J. Yang, Y. Hu, G. Zhang, Y. Wang, F. Zhao, G. Hao and W. Jiang, *Def. Technol.*, 2023, **19**, 163–195.

26 M. Rahm and T. Brinck, *Chem. Phys.*, 2008, **348**, 53–60.

27 Y. I. Izato and A. Miyake, *J. Energ. Mater.*, 2018, **36**, 302–315.

28 S. Tian, Y. Wang, X. Chen, D. Hu, Y. Hu, S. Zheng, Z. Zhou, C. Xiao and Z. Ren, *Propellants, Explos., Pyrotech.*, 2023, **48**, e202200344.

29 H. Yang, F. Chen, Y. Hu, Q. Lu, L. Xiao, Y. Wang, F. Zhao, W. Jiang and G. Hao, *Def. Technol.*, 2023, DOI: 10.1016/j.dt.2023.08.012.

30 P. Kumar, *Def. Technol.*, 2018, **14**, 661–673.

31 X. Ma, S. Jin, W. Xie, Y. Liu, W. Zhang and Y. Chen, *Colloids Surf., A*, 2022, **641**, 128550.

32 Y. Hou, Y. Yu, X. Liu, J. Chen and T. Zhang, *ACS Omega*, 2021, **6**, 22937–22944.

33 F. Wang, S. Zhang, X. Yu, X. Lin, J. Li and Y. Liu, *J. Anal. At. Spectrom.*, 2021, **36**, 1996–2006.

34 L. Jing, X. You, J. Huo, M. Zhu and Z. Yao, *Aerosp. Sci. Technol.*, 2017, **69**, 161–170.

35 J. Cheng, J. Cao, F. Li, Z. Zhang, J. Xu, K. Ouyang, C. Rossi, Y. Ye and R. Shen, *Chem. Eng. J.*, 2023, 144412.

© 2024 The Author(s). Published by the Royal Society of Chemistry

36 J. Li, W. Tang, Z. Liu, K. Cong, L. Gong, J. Li and R. Yang, *J. Alloys Compd.*, 2022, **907**, 164349.

37 A. Nosseir, A. Cervone and A. Pasini, *Aerospace*, 2021, **8**, 20.

38 D. Lee, J. Kim and S. Kwon, *Sens. Actuators, A*, 2018, **283**, 211–219.

39 D. Freudenmann and H. K. Ciezki, *Propellants, Explos., Pyrotech.*, 2019, **44**, 1084–1089.

40 M. Negri, M. Wilhelm and H. K. Ciezki, *Propellants, Explos., Pyrotech.*, 2019, **44**, 1096–1106.

41 J. Shen, Y. Yu, X. Liu and J. Cao, *Micromachines*, 2022, **13**, 510.

42 J. Chen, G. Li, T. Zhang, Y. Liu, R. Yang and Y. Chen, *Chin. J. Chem. Eng.*, 2019, **27**, 1159–1165.

43 F. Wang, S. Zhang and X. Yu, *Spectrochim. Acta, Part B*, 2023, **200**, 106589.

44 Y. Hou, Y. Yu, X. Liu and J. Cao, *Micromachines*, 2022, **13**, 605.

45 L. Jing, J. Huo, H. Wang, X. You, M. Zhu, Y. Yang and Z. Yao, *J. Propul. Power*, 2017, **33**, 343–349.

46 M. Persson, K. Anflo and P. Friedhoff, *Propellants, Explos., Pyrotech.*, 2019, **44**, 1073–1079.

47 J. Kleimark, R. Delanoë, A. Demairé and T. Brinck, *Theor. Chem. Acc.*, 2013, **132**, 1–9.

48 N. E. Ermolin and V. M. Fomin, *Combust., Explos. Shock*, 2016, **52**, 566–586.

49 T. Zhang, F. Wang and J. Chen, *J. Therm. Sci.*, 2020, **29**, 81–89.

50 P. Thakre, Y. Duan and V. Yang, *Combust. Flame*, 2014, **161**, 347–362.

51 H. Matsunaga, H. Habu and A. Miyake, *J. Therm. Anal. Calorim.*, 2013, **113**, 1387–1394.

52 T. Zeng, R. Yang, D. Li, J. Li, X. Guo and P. Luo, *Propellants, Explos., Pyrotech.*, 2020, **45**, 1590–1599.

53 I. B. Mishra and T. Russell, *Thermochim. Acta*, 2002, **384**, 47–56.

54 R. J. Doyle Jr, *Org. Mass Spectrom.*, 1993, **28**, 83–91.

55 Q. Lu, F. Chen, L. Xiao, J. Yang, Y. Hu, G. Zhang, F. Zhao, Y. Wang, W. Jiang and G. Hao, *Mater. Today Commun.*, 2022, **31**, 103699.

56 A. Snelson and A. Tulis, *Nineteenth Intern. Pyrotechnics Seminar*, Christchurch, New Zeland, 1994, pp. 20–25.

57 R. S. Zhu, H. L. Chen and M. C. Lin, *J. Phys. Chem. A*, 2012, **116**, 10836–10841.

58 K. Wang, B. Xue, J.-G. Chen, Z.-H. He, Y. Ji, B. Wang, J. Lu, Z.-W. Liu and Z.-T. Liu, *New J. Chem.*, 2020, **44**, 6833–6844.

59 A. M. Mebel, M. C. Lin, K. Morokuma and C. F. Melius, *J. Phys. Chem.*, 1995, **99**, 6842–6848.

60 J. Oxley, J. Smith, W. Zheng, E. Rogers and M. Coburn, *J. Phys. Chem. A*, 1997, **101**, 5646–5652.

61 R. Yang, P. Thakre and V. Yang, *Combust., Explos. Shock*, 2005, **41**, 657–679.

62 B. L. Fetherolf and T. A. Litzinger, *Combust. Flame*, 1998, **114**, 515–530.

63 S. Vyazovkin and C. A. Wight, *J. Phys. Chem. A*, 1997, **101**, 7217–7221.

64 S. Vyazovkin and C. A. Wight, *J. Phys. Chem. A*, 1997, **101**, 5653–5658.

65 K. Fujisato, H. Habu and K. Hori, *Propellants, Explos., Pyrotech.*, 2014, **39**, 714–722.

66 F. Dubovitskii, G. Volkov, V. Grebennikov, G. Manelis and G. Nazin, *Dokl. Chem.*, 1996, 106–108.

67 A. P. Vandel', A. A. Lobanova and V. S. Loginova, *Russ. J. Appl. Chem.*, 2009, **82**, 1763.

68 S. Löbbecke, H. H. Krause and A. Pfeil, *Propellants, Explos., Pyrotech.*, 1997, **22**, 184–188.

69 S. Löbbecke, T. Keicher, H. Krause and A. Pfeil, *Solid State Ionics*, 1997, **101**, 945–951.

70 P. Politzer and J. M. Seminario, *Chem. Phys. Lett.*, 1993, **216**, 348–352.

71 M. Rahm and T. Brinck, *Chem. Commun.*, 2009, 2896–2898.

72 Y. I. Izato and A. Miyake, *Combust. Flame*, 2018, **198**, 222–229.

73 N. V. Muravyev, K. A. Monogarov, A. A. Bragin, I. V. Fomenkov and A. N. Pivkina, *Thermochim. Acta*, 2016, **631**, 1–7.

74 N. V. Muravyev, N. Koga, D. B. Meerov and A. N. Pivkina, *Phys. Chem. Chem. Phys.*, 2017, **19**, 3254–3264.

75 H. Matsunaga, H. Habu and A. Miyake, *J. Therm. Anal. Calorim.*, 2013, **111**, 1183–1188.

76 P. Kumar, R. Kumar and P. C. Joshi, *Proceedings of the International Conference on Modern Research in Aerospace Engineering: MRAE-2016*, Springer, 2018, pp. 1–11.

77 J. C. Oxley, J. L. Smith, E. Rogers and M. Yu, *Thermochim. Acta*, 2002, **384**, 23–45.

78 R. Turcotte, P. Lightfoot, R. Fouchard and D. Jones, *J. Hazard. Mater.*, 2003, **101**, 1–27.

79 P. Kumar, P. C. Joshi and R. Kumar, *Combust. Flame*, 2016, **166**, 316–332.

80 M. Yang, X. Chen, Y. Wang, B. Yuan, Y. Niu, Y. Zhang, R. Liao and Z. Zhang, *J. Hazard. Mater.*, 2017, **337**, 10–19.

81 M. Abd-Elghany, A. Elbeih and T. M. Klapötke, *J. Anal. Appl. Pyrolysis*, 2018, **133**, 30–38.

82 J. Meng, Y. Pan, Z. Ran, Y. Li, J. Jiang, Q. Wang and J. Jiang, *J. Loss Prev. Process Ind.*, 2021, **72**, 104562.

83 Y. Li, W. Xie, H. Wang, H. Yang, H. Huang, Y. Liu and X. Fan, *Propellants, Explos., Pyrotech.*, 2020, **45**, 1607–1613.

84 R. Eloirdi, S. Rossignol, C. Kappenstein, D. Duprez and N. Pillet, *J. Propul. Power*, 2003, **19**, 213–219.

85 R. Amrousse, K. Hori, W. Fetimi and K. Farhat, *Appl. Catal., B*, 2012, **127**, 121–128.

86 L. Courtheoux, E. Gautron, S. Rossignol and C. Kappenstein, *J. Catal.*, 2005, **232**, 10–18.

87 M. Kurt, Z. Kap, S. Senol, K. E. Ercan, A. T. Sika-Nartey, Y. Kocak, A. Koc, H. Esiyok, B. S. Caglayan, A. E. Aksoylu and E. Ozensoy, *Appl. Catal., A*, 2022, **632**, 118500.

88 S. Li, H. Yan, Z. Wang, Y. Tang, Z. Yao and S. Li, *Energy Fuels*, 2021, **35**, 18716–18725.

89 J. Kim, Y. Jo, J. Jeon and T. Kim, *J. Nanosci. Nanotechnol.*, 2020, **20**, 5780–5782.

90 Y. Batonneau, R. Brahmi, B. Cartoixa, K. Farhat, C. Kappenstein, S. Keav, G. Kharchafi-Farhat, L. Pirault-Roy, M. Saouabé and C. Scharlemann, *Top. Catal.*, 2014, **57**, 656–667.

91 J. Lin, L. Li, X. Pan, X. Wang, Y. Cong, T. Zhang and S. Zhu, *AIChE J.*, 2016, **62**, 3973–3981.

92 J. X. Zhai, R. J. Yang, J. M. Li and X. D. Li, *Chin. J. Energ. Mater.*, 2005, **13**, 397–400.

93 X. D. Li and R. J. Yang, *New Carbon Mater.*, 2010, **25**, 444–448.

94 H. Z. Duan, Q. L. Li and D. B. Liu, *International Seminar on Propellants, Explosives and Pyrotechnics*, Nanjing, China, 2011.

95 C. Shamjitha and A. A. Vargeese, *Def. Technol.*, 2023, DOI: 10.1016/j.dt.2023.05.007.

96 K. Fujisato, H. Habu, A. Miyake, K. Hori and A. B. Vorozhtsov, *Propellants, Explos., Pyrotech.*, 2014, **39**, 518–525.

97 H. Matsunaga, Y.-i. Izato, H. Habu and A. Miyake, *J. Therm. Anal. Calorim.*, 2015, **121**, 319–326.

98 R. Gugulothu, A. K. Macharla, K. Chatragadda and A. A. Vargeese, *Thermochim. Acta*, 2020, **686**, 178544.

99 X. Lu, W. Cong, B. Hou, S. Zhu and X. Wang, *Chem. Eng.*, 2017, **45**, 61–64.

100 S. Baek, M. Monette, Y. S. Jung, J. Kim, W. Kim, Y. Jo, H. Yoon, J. Lee and S. Kwon, *Proceedings of the Korean Society of Propulsion Engineers Conference*, 2017, pp. 739–745.

101 C. Maleix, P. Chabernaud, R. Brahmi, R. Beauchet, Y. Batonneau, C. Kappenstein, M. Schwentenwein, R.-J. Koopmans, S. Schuh and C. Scharlemann, *Acta Astronaut.*, 2019, **158**, 407–415.

102 D. Hochfilzer, I. Chorkendorff and J. Kibsgaard, *ACS Energy Lett.*, 2023, **8**, 1607–1612.

103 M. Tawalbeh, R. M. N. Javed, A. Al-Othman and F. Almomani, *Energy Convers. Manage.*, 2023, **279**, 116755.

104 K. Liu, S. Yang, W. Li, Y. Wang, C. Sun, L. Peng and H. Garcia, *Fuel*, 2023, **337**, 126840.

105 A. R. Sudhakar and S. Mathew, *Thermochim. Acta*, 2006, **451**, 5–9.

106 A. A. Vargeese and K. Muralidharan, *Appl. Catal., A*, 2012, **447–448**, 171–177.

107 K. Kajiyama, Y.-i. Izato and A. Miyake, *J. Therm. Anal. Calorim.*, 2013, **113**, 1475–1480.

108 Q. Li, Q. Zhang, W. Xu, R. Zhao, M. Jiang, Y. Gao, W. Zhong, K. Chen, Y. Chen and X. Li, *Adv. Energy Mater.*, 2023, **13**, 2203955.

109 R. Xiao, J. Jia, R. Wang, Y. Feng and H. Chen, *Acc. Chem. Res.*, 2023, **56**, 1539–1552.

110 L. Y. Zhu, L. X. Ou, L. W. Mao, X. Y. Wu, Y. P. Liu and H. L. Lu, *Nano-Micro Lett.*, 2023, **15**, 89.

111 K. Farhat, C. Kappenstein and Y. Batonneau, *44th AIAA/ASME/SAE/ASEE Joint Propulsion Conference & Exhibit*, 2008, p. 4938.

112 K. Farhat, W. Cong, Y. Batonneau and C. Kappenstein, *45th AIAA/ASME/SAE/ASEE Joint Propulsion Conference & Exhibit*, 2009, p. 4963.

113 S. Hong, S. Heo, C. Li, B. K. Jeon, J. M. Kim, Y. M. Jo, W. Kim and J.-K. Jeon, *J. Nanosci. Nanotechnol.*, 2018, **18**, 1427–1430.

114 W. Yoon, V. K. Bhosale and H. Yoon, *Aerospace*, 2023, **10**, 686.

115 S. Hu and W. X. Li, *Science*, 2021, **374**, 1360–1365.

116 T. W. van Deelen, C. Hernández Mejía and K. P. de Jong, *Nat. Catal.*, 2019, **2**, 955–970.

117 B. R. Goldsmith, B. Peters, J. K. Johnson, B. C. Gates and S. L. Scott, *ACS Catal.*, 2017, **7**, 7543–7557.

118 J. Yang, Q. Wang, T. Wang and Y. Liang, *RSC Adv.*, 2016, **6**, 26271–26279.

119 F. Rascón, R. Wischert and C. Copéret, *Chem. Sci.*, 2011, **2**, 1449–1456.

120 W. Huang, G. Liu, X. Li, T. Qi, Q. Zhou and Z. Peng, *J. Alloys Compd.*, 2020, **824**, 153905.

121 C. Maleix, P. Chabernaud, M. Artault, R. Brahmi and C. Kappenstein, *53rd AIAA/SAE/ASEE Joint Propulsion Conference*, 2017.

122 M. Kim, D. Yoo, J. Lee and J. K. Joen, *Korean Chem. Eng. Res.*, 2021, **59**, 296–303.

123 M. V. Bukhtiyarova, A. S. Ivanova, G. S. Litvak and L. M. Plyasova, *Kinet. Catal.*, 2009, **50**, 824–829.

124 R. Kuzmin, N. Cherkasova, A. Bataev, S. Veselov, T. Ogneva, A. Ruktuev and A. Felofyanova, *Ceram. Int.*, 2021, **47**, 6854–6859.

125 N. Cherkasova, S. Veselov, A. Bataev, R. Kuzmin and N. Stukacheva, *Mater. Chem. Phys.*, 2021, **259**, 123938.

126 J. Heveling, *Ind. Eng. Chem. Res.*, 2023, **62**, 2353–2386.

127 J. J. Torrez-Herrera, S. A. Korili and A. Gil, *Catal. Rev.*, 2022, **64**, 592–630.

128 H. Jo, D. You, M. Kim, J. Woo, K. Y. Jung, Y. M. Jo and J. K. Jeon, *Clean Technol.*, 2018, **24**, 371–379.

129 S. Hong, S. Heo, W. Kim, Y. M. Jo, Y. K. Park and J. K. Jeon, *Catalysts*, 2019, **9**, 80.

130 S. Heo, M. Kim, J. Lee, Y. C. Park and J. K. Jeon, *Korean J. Chem. Eng.*, 2019, **36**, 660–668.

131 Z. Li, S. Zhao, R. O. Ritchie and M. A. Meyers, *Prog. Mater. Sci.*, 2019, **102**, 296–345.

132 L. Yang, H. Qian and W. Kuang, *Materials*, 2022, **15**, 1331.

133 U. Gotzig, *7th European Conference for Aeronautics and Space Sciences (EUCASS)*, 2017.

134 M. Wilhelm, M. Negri, H. Ciezki and S. Schlechtriem, *Acta Astronaut.*, 2019, **158**, 388–396.

135 L. Li, G.-X. Li, H.-M. Li, Z.-P. Yao and T. Zhang, *Sci. Technol. Energ. Mater.*, 2023, **84**, 72–79.

136 B. Du, Y. Zheng, C. Mao, H. Cui, J. Han, L. Jiang, J. Ye and Y. Hong, *Micromachines (Basel)*, 2023, **14**, 1219.

137 T. Zhang, G. Li, Y. Yu, Z. Sun, M. Wang and J. Chen, *Energy Convers. Manage.*, 2014, **87**, 965–974.